

## 1.42 Å crystal structure of mini-IGF-1(2): an analysis of the disulfide isomerization property and receptor binding property of IGF-1 based on the three-dimensional structure<sup>☆</sup>

Cai-Hong Yun<sup>a</sup>, Yue-Hua Tang<sup>b</sup>, You-Min Feng<sup>b</sup>, Xiao-Min An<sup>a</sup>,  
Wen-Rui Chang<sup>a</sup>, Dong-Cai Liang<sup>a,\*</sup>

<sup>a</sup> National Key Laboratory of Biomacromolecules, Institute of Biophysics, Chinese Academy of Sciences, 15 Datun Road, Chaoyang District, Beijing 100101, PR China

<sup>b</sup> State Key Laboratory of Molecular Biology, Institute of Biochemistry and Cell Biology, Shanghai Institutes for Biological Sciences, Chinese Academy of Sciences, 320 Yue-yang Road, Shanghai 200031, PR China

Received 24 October 2004

### Abstract

Insulin and insulin-like growth factor 1 (IGF-1) share a homologous sequence, a similar three-dimensional structure and weakly overlapping biological activity, but IGF-1 folds into two thermodynamically stable disulfide isomers, while insulin folds into one unique stable tertiary structure. This is a very interesting phenomenon in which one amino acid sequence encodes two three-dimensional structures, and its molecular mechanism has remained unclear for a long time. In this study, the crystal structure of mini-IGF-1(2), a disulfide isomer of an artificial analog of IGF-1, was solved by the SAD/SIRAS method using our in-house X-ray source. Evidence was found in the structure showing that the intra-A-chain/domain disulfide bond of some molecules was broken; thus, it was proposed that disulfide isomerization begins with the breakdown of this disulfide bond. Furthermore, based on the structural comparison of IGF-1 and insulin, a new assumption was made that in insulin the several hydrogen bonds formed between the N-terminal region of the B-chain and the intra-A-chain disulfide region of the A-chain are the main reason for the stability of the intra-A-chain disulfide bond and for the prevention of disulfide isomerization, while Phe B1 and His B5 are very important for the formation of these hydrogen bonds. Moreover, the receptor binding property of IGF-1 was analyzed in detail based on the structural comparison of mini-IGF-1(2), native IGF-1, and small mini-IGF-1.

© 2004 Elsevier Inc. All rights reserved.

**Keywords:** IGF; Crystal structure; Disulfide isomerization; Protein folding; Receptor binding

Insulin-like growth factor 1 (IGF-1) is a member of the insulin superfamily. It is a key regulator of cell proliferation, differentiation, and transformation, and is thus pivotal in the occurrence of several kinds of cancers [1,2]. It also has some metabolic regulation activity like that of insulin [3].

IGF-1 and insulin share a homologous sequence, a similar three-dimensional structure, and weakly overlapping biological activity, but their folding behavior is different. IGF-1 is a 70 residue single-chain globular protein composed of B-, C-, A-, and D-chains/domains from the N-terminus to the C-terminus (Fig. 1). The B-chain/domain consists of 29 residues, which is homologous to the B-chain of insulin (residues 2–30); the C-chain/domain consists of 12 residues, which is analogous to the C-peptide of proinsulin, but they share no homology; the A-chain/domain consists of 21 residues,

<sup>☆</sup> PDB reference: Crystal Structure of mini-IGF-1(2), 1TGR.

\* Corresponding author. Fax: +86 10 64889867.

E-mail address: [dcliang@sun5.ibp.ac.cn](mailto:dcliang@sun5.ibp.ac.cn) (D.-C. Liang).

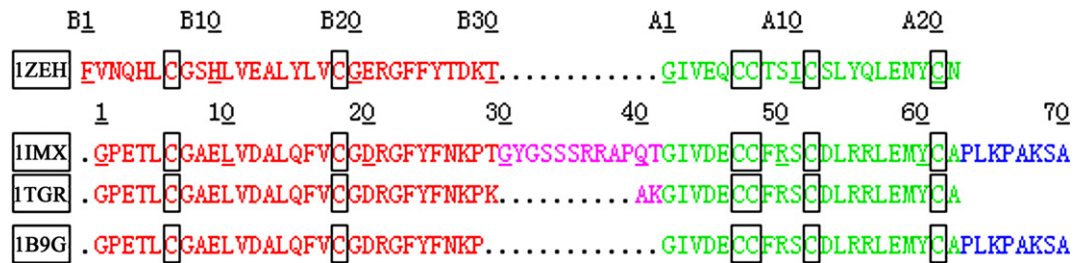


Fig. 1. Sequence alignment of insulin (I<sub>ZEH</sub>), IGF-1 (I<sub>IMX</sub>), mini-IGF-1(2) (I<sub>TGR</sub>), and small mini-IGF-1 (I<sub>B9G</sub>).

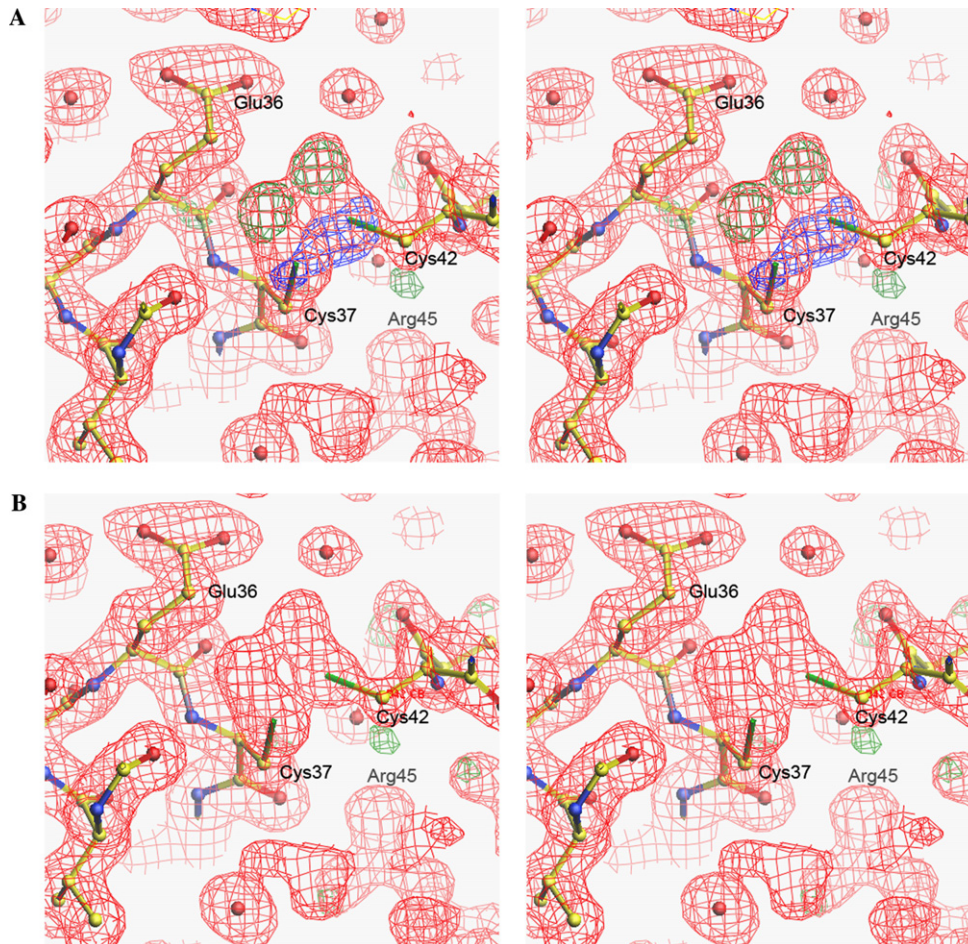


Fig. 2. Stereo views showing the electron density of the Cys37–Cys42 disulfide bond and the adjacent area in molecule II. Because of the obvious conformational instability, the electron density of this region is dispersive. (A) The electron density maps were calculated using a refined model in which Glu36 had only one conformation, and the occupancy of the S atoms was set at 1.00. (B) The electron density maps were calculated using a refined model in which the Glu36 residue was built as two alternative conformations (in the minor conformation, the carboxylate O atoms occupy the “extra” electron density beside the disulfide bond), and the occupancy of the S atoms was set at 0.50. The red line indicates the  $2F_o - F_c$  map (contoured at  $1.0\sigma$ ), the green line indicates the  $4.5\sigma$  positive  $F_o - F_c$  electron density, and the blue line indicates the  $-4.5\sigma$  negative  $F_o - F_c$  electron density. (For interpretation of the references to colour in this figure legend, the reader is referred to the web version of this paper.)

which is homologous to the A-chain of insulin; and the D-chain/domain is an 8-residue peptide that has no counterpart in insulin. IGF-1 can fold into two thermodynamically stable disulfide isomers, unlike insulin, which only folds into one thermodynamically stable structure. One of the two IGF-1 isomers is called native IGF-1, and its disulfide pairing is Cys47–Cys52, Cys6–

Cys48, and Cys18–Cys61, which is the same as that of insulin (Cys A6–Cys A11, Cys A7–Cys B7, and Cys A20–Cys B19); the other one is called swap IGF-1, which has a swapped disulfide pairing style (Cys48–Cys52, Cys6–Cys47, and Cys18–Cys61). Why does the folding behavior of the two proteins differ so much and how does the amino acid sequence of IGF-1 encode

two kinds of three-dimensional structures? These questions have interested scientists for a long time. DiMarchi et al. [4] have demonstrated that it is the A- and B-chains/domains that drive IGF-1 to fold into two disulfide isomers. In order to further elucidate the molecular mechanism, Guo et al. [5] prepared two single chain hybrids of mini-IGF-1 and porcine insulin precursor (PIP): Ins(A)/IGF-1(B) and Ins(B)/IGF-1(A). In PIP the A-chain and B-chain of porcine insulin were linked by a two-residue peptide, AK, which was the same as the linker peptide used to connect the B-chain/domain and A-chain/domain of IGF-1 in the mini-IGF-1 molecule. PIP folds into only one thermodynamically stable tertiary structure just like that of insulin. It was found that Ins(A)/IGF-1(B) folds into two kinds of thermodynamically stable three-dimensional structures just like that of IGF-1/mini-IGF-1, while Ins(B)/IGF-1(A) folds into only one unique thermodynamically stable structure like that of PIP/insulin, thus demonstrating that it is the B-chain/domain that determines the different folding behavior of insulin and IGF-1.

The receptor binding property of IGF-1 is similar to that of insulin, but not exactly the same. IGF-1 can bind to the type 1 IGF receptor (IGF-1R) with high affinity and to the insulin receptor (IR) with lower affinity [6,7]. Similarly, insulin also can bind to IGF-1R with lower affinity. The reason that insulin has some growth-promoting activity and IGF-1 has some metabolic regulation activity may be that they can cross bind to each other's receptors. Research on the receptor binding mechanism of insulin has a long history, and relatively mature models have been proposed for the receptor binding sites and receptor binding induced conformational change [3,8–11], while research on IGF-1's receptor binding mechanism has not been as thorough, and the main achievement has been the identification of some key residues for receptor binding in IGF-1 based on site-directed mutagenesis [12,13]. Although a model similar to that of insulin has been proposed for the conformational change of IGF-1 when it binds to its receptor [14], this point may need more experimental proof to make it compelling, because IGF-1's receptor

binding mechanism is not the same as that of insulin. For example, it is well known that there is a key residue for receptor binding in the C-chain/domain of IGF-1 [13], which is impossible in insulin.

Mini-IGF-1 is an analog designed by Feng et al. that consists of 52 residues (Fig. 1). The previously reported mini-IGF-1 made by Wolf et al. [15] is called “small mini-IGF-1” in this paper (Fig. 1). Similar to IGF-1, mini-IGF-1 also folds into two thermodynamically stable disulfide isomers: mini-IGF-1(1) and mini-IGF-1(2). Of these, mini-IGF-1(2) was thought to have the native disulfide pairing and mini-IGF-1(1) was thought to have the swapped disulfide pairing [5]. In order to prove the disulfide pairing style of mini-IGF-1(2), to provide a detailed analysis of the reason for disulfide isomerization, and to further study the structural basis for receptor binding of IGF-1, the crystal structure of mini-IGF-1(2) was solved.

## Materials and methods

**Crystallization, derivative preparation, and data collection.** Mini-IGF-1(2) was crystallized by the hanging drop vapor diffusion method. The crystallization condition was as follow: 0.5 ml solution I (0.1 M citrate buffer, pH 6.65, 1.0 M NaCl, 12% (v/v) ethanol, and 5 mM  $\text{Zn}(\text{CH}_3\text{COO})_2$ ) was taken as the reservoir, and the hanging drop mixture was made by mixing 1  $\mu\text{l}$  protein solution (8 mg/ml mini-IGF-1(2), dissolved in 0.005 M HCl) and 1  $\mu\text{l}$  modified reservoir solution (14% instead of 12% ethanol was used here). The crystallization was performed under a constant temperature of 16 °C.

The Gd-DTPA derivative was made by the method of Girard et al. [16]. The native and derivative datasets used in phasing were both collected on our in-house Cu-anode X-ray source and Mar345 IP detector, and the total oscillation angle used for collecting the derivative dataset was 366°. The dataset used in structure refinement was collected on the BL6B beamline (the Photon Factory, Tsukuba, Japan). All the datasets were collected under the cryogenic temperature of 100 K. The data were processed and scaled with *DENZO* and *SCALEPACK* [17]. The mini-IGF-1(2) crystals belong to space group  $I222$  or  $I2_12_12_1$  with cell parameters of  $a = 58.9 \text{ \AA}$ ,  $b = 62.0 \text{ \AA}$ , and  $c = 70.8 \text{ \AA}$ , and there are two mini-IGF-1(2) molecules in the asymmetric unit. The statistics of these three datasets are summarized in Table 1.

**Structure determination and refinement.** The crystal structure of mini-IGF-1(2) can be successfully determined by the SAD or SIRAS

Table 1  
Diffraction dataset statistics of mini-IGF-1(2) crystals

Statistics	Native dataset	Derivative dataset	High resolution native dataset
Wavelength (Å)	1.5418	1.5418	1.0000
Resolution (Å)	1.87	2.65	1.42
Total reflections	1,05,662	96,064	2,23,072
Unique reflections	10,694	3940	23,375
Completeness (%)	98.2 (87.4)	99.8 (98.8)	99.6 (100.0)
$I/\sigma$	18.8 (2.2)	25.4 (6.9)	16.7 (4.6)
$R_{\text{merge}}(\%)$	8.0 (34.4)	11.2 (37.4)	9.6 (37.6)

Values in parentheses are for the highest resolution shell: native dataset, 1.91–1.87 Å; derivative dataset, 2.73–2.65 Å; and high resolution native dataset, 1.45–1.42 Å.



method. First, the difference Patterson map was calculated and the space group was determined as *I*222 according to the pattern of the Harker peaks of the heavy atom, and the position of this heavy atom was determined. Then the heavy atom parameters were refined and the initial phase angles were calculated using SHARP [18]. In the anomalous residual map [18], two additional minor anomalous scatters were found, which were later identified as the Cys6–Cys38 disulfide bond of the two molecules, but they were not included in phasing because they were weak. After refinement, SHARP reported that the occupancy of the heavy atom was 0.20, and the calculated experimental phase had an overall figure of merit of 0.45 (acentric reflections) and 0.59 (centric reflections) for 25–3.0 Å diffraction data. After the phase improvement was made mainly using SOLOMON [19], the overall figure of merit increased to 0.88, and the quality of the electron density map was improved substantially.

ARP/wARP was used to automatically build the model in the 1.87 Å electron density map [20], and 98 residues out of the total 104 residues were correctly built. After the automatic model building, an artificial model check and rebuilding was performed. It was found that the main-chain of all the 104 residues could be clearly determined and the electron density of the side-chains of most residues was good, with the exception of several residues located on the N-terminal end of the two molecules. After model building, the model was refined with REFMAC5 using the 1.42 Å high-resolution dataset [21]. O was used to artificially adjust the model between the big REFMAC5 cycles [22], and ARP\_WATERS combined with the artificial check method was used in building the water molecules in the final steps [20].

Table 2  
Structural and refinement statistics

Resolution range (Å)	8.0–1.42
Total reflections (completeness)	23,375 (99.95%)
Reflections used for cross validation	1262
Number of total non-hydrogen atoms	810
Number of water molecules	145
<i>R</i>	0.196
<i>R</i> <sub>free</sub>	0.224
Stereo-chemistry properties of the final model	
RMSD bond length (Å)	0.016
RMSD bond angle (°)	1.6
Ramachandran plot (%)	
Most favored regions	98.90
Additional allowed regions	1.10
Generously allowed regions	0
Disallowed regions	0
Average <i>B</i> factor (Å <sup>2</sup> )	20.8
Main-chain atoms	17.7 (11.6–33.7)
Side-chain atoms	19.8 (10.2–37.5)
Water atoms	33.1 (16.3–47.8)

Table 3  
The difference between the helix backbone in mini-IGF-1(2) and in native IGF-1

	Residue number		Number of residues		Type of helix	
	Mini-IGF-1(2)	IGF-1	Mini-IGF-1(2)	IGF-1	Mini-IGF-1(2)	IGF-1
B-chain						
Helix I	4–18	7–18	15	12	α-Helix	α-Helix
A-chain						
Helix II	27–37	43–47	11	5	α-Helix	α-Helix
Helix III	44–50	54–58	7	5	3 <sub>10</sub> -Helix	α-Helix

## Results and discussion

### Crystal structure of mini-IGF-1(2)

The structural and refinement statistics of mini-IGF-1(2) are summarized in Table 2.

Mini-IGF-1(2) is mainly composed of three helices, which are similar to those of native IGF-1, but the length, type, and relative position of these helices are quite different (Table 3). The differences are especially great for helix II, which is located in the N-terminal region of the A-chain/domain of IGF-1. In mini-IGF-1(2) it extends and forms an elongated α-helix with the linker peptide (two residues) and three residues in the C-terminal end of the B-chain/domain including a Pro residue. Thus, helix II in mini-IGF-1 is twice as long as that in IGF-1. And their helix III differs from each other not only in length, but also in type.

### An analysis of the disulfide isomerization properties of IGF-1

The disulfide isomerization of IGF-1 has interested researchers for many years. Mini-IGF-1 also has a disulfide isomerization behavior like that of IGF-1, so we analyzed the structural basis for disulfide isomerization of mini-IGF-1 intensively.

### The disulfide isomerization perhaps begins with the break down of the intra-A-chain/domain disulfide bond

The electron density of the intra-A-chain/domain disulfide (Cys37–Cys42) of the second molecule in the asymmetric unit of mini-IGF-1(2) is unusual (Fig. 2). There are two strong positive peaks about 1.4–1.7 Å away from the S atoms in the  $F_o - F_c$  electron density map. Although the two S atoms adapt to the  $2F_o - F_c$  map quite well, there is also strong negative  $F_o - F_c$  electron density at the same position. The negative  $F_o - F_c$  electron density of the two S atoms cannot be eliminated unless their occupancies are set to less than 1.00 (e.g., 0.50), which indicates that the disulfide bond may not be the only conformation. The electron density of the environmental part including the backbone is more dispersed than the other part of the model, which

also indicates that the conformation of this part may be unstable.

It was deduced that the strange electron density is caused by the instability of the conformation in this region. The carboxylate O atoms of Glu36 can occupy the “extra” electron density beside the disulfide bond if the side chain of Glu36 swings to the disulfide bond. However, serious close contact will occur if the disulfide bond still exists when the side-chain of Glu36 swings to this position. Taking into account the facts that the occupancy of the two S atoms of the Cys37–Cys42 disulfide bond should be lower than 1.00 and that the electron density of this area is relatively dispersive, we deduced that this disulfide bond was broken in some molecule IIs, and in these molecules with broken Cys37–Cys42 disulfide bonds, the side-chain of Glu36 may swing to the position of the disulfide bond. The position of the two Cys residues after the break down of the disulfide could not be identified in the electron density map. This may be because there are not many molecules with broken Cys37–Cys42 disulfide bonds and because this part of the molecule may become much more flexible after the break down of the disulfide bond.

The electron density of all the other disulfide bonds (three disulfide bonds in molecule I and the other two disulfide bonds in molecule II) are normal. So it is believed that only a small quantity of molecule IIs have broken Cys37–Cys42 disulfide bonds. Thus, we deduced that the disulfide isomerization of mini-IGF-1(2) begins with the break down of this intra-A-chain/domain disulfide bond. In fact, this disulfide bond is an unstable bond with high energy [23]. The work of Guo et al. [24] has demonstrated that the different energetic state of the intra-A-chain/domain disulfide bond of insulin and IGF-1 is mainly controlled by their B-chain/domain.

*The determinant for the instability of the intra-A-chain/domain disulfide bond and the disulfide isomerization of the molecule may be the residues in the N-terminal region of the B-chain/domain*

It is still not known why the B-chain/domain can determine the stability of the intra-A-chain/domain disulfide bond nor is it known which residues in the B-chain/domain determine this. Three-dimensional structural comparison of IGF-1, mini-IGF-1, and insulin may answer these questions.

It was found that in the insulin structure (molecule II of two zinc porcine insulin, PDB ID: 4INS [25]. The conformation of this molecule is generally believed to represent the conformation of the natural insulin monomer in circulation.), the N-terminus of the B-chain/domain runs backward and close to the A-chain/domain, and several hydrogen bonds are formed between the main-chain O or N atoms of residues A6–A11 and the

Table 4

The hydrogen bonds formed between residues A6–A11 and the B-chain/domain in insulin

Hydrogen bond donor	Hydrogen bond acceptor	Bond length (Å)
Gln B4, N	Cys A11, O	3.1
Cys A11, N	Gln B4, O	3.2
His B5, ND1	Ser A9, O	2.9
His B5, ND1	Cys A7, O	2.9
Leu B6, N	Cys A6, O	2.8

main-chain N or O atoms of residues B1–B7 as well as the side-chain N atom of His B5 (Table 4, Fig. 3A). These hydrogen bonds stabilize the conformation of the intra-A-chain disulfide region of the A-chain/domain. In the same region of IGF-1 and mini-IGF-1(2), such hydrogen bonds do not exist (Fig. 3B), so their intra-A-chain disulfide bond is not as stable as that of insulin.

It was deduced that residues Phe B1 and His B5 in insulin play important roles in the formation of these hydrogen bonds. The hydrophobic side-chain of Phe B1 can easily interact with the partially exposed hydrophobic core of the molecule made by Leu A13, Leu B17, and Val B18, etc., thus driving the N-terminus of the B-chain/domain backward and close to the A-chain to make the hydrogen bonds available, while the N atom of the side-chain of His B5 makes two strong hydrogen bonds with the main-chain O atoms of Cys A7 and Cys A9. At the N-terminal end of the B-chain/domain of IGF-1 and mini-IGF-1, there is no large hydrophobic residue like Phe, so there is no appropriate hydrophobic interaction to bind up the N-terminus of the B-chain/domain, and thus the hydrogen bonds between the main-chain atoms of the A-chain/domain and B-chain/domain cannot be formed easily. Furthermore, the counterpart of His B5 in insulin is Thr4 in IGF-1 and mini-IGF-1, which is a weaker hydrogen bond donor than His. For these reasons we deduced that Phe B1 and His B5 mainly determine the absence of disulfide isomerization of the molecule. This conclusion is consistent with Chen et al.’s report [26]. They constructed [1–9]PIP (residues 1–10 of PIP were replaced by residues 1–9 of IGF-1) and [1–10]mini-IGF-1 (residues 1–9 of mini-IGF-1 were replaced by residues 1–10 of PIP), and demonstrated that [1–10]mini-IGF-1 folds into one unique thermodynamically stable structure like PIP/insulin, while [1–9]PIP folds into two kinds of thermodynamically stable structures. These results indicate that residues 1–10/1–9 of the B-chain/domain constitute the molecular basis of the different folding behavior of insulin and IGF-1. Amphioxus insulin-like peptide (aILP) is the common ancestor of insulin and IGF-1. Wang et al. [27] studied the in vitro folding of aILP, and their results indicated that the different folding behavior of insulin and IGF-1 could be attributed to a

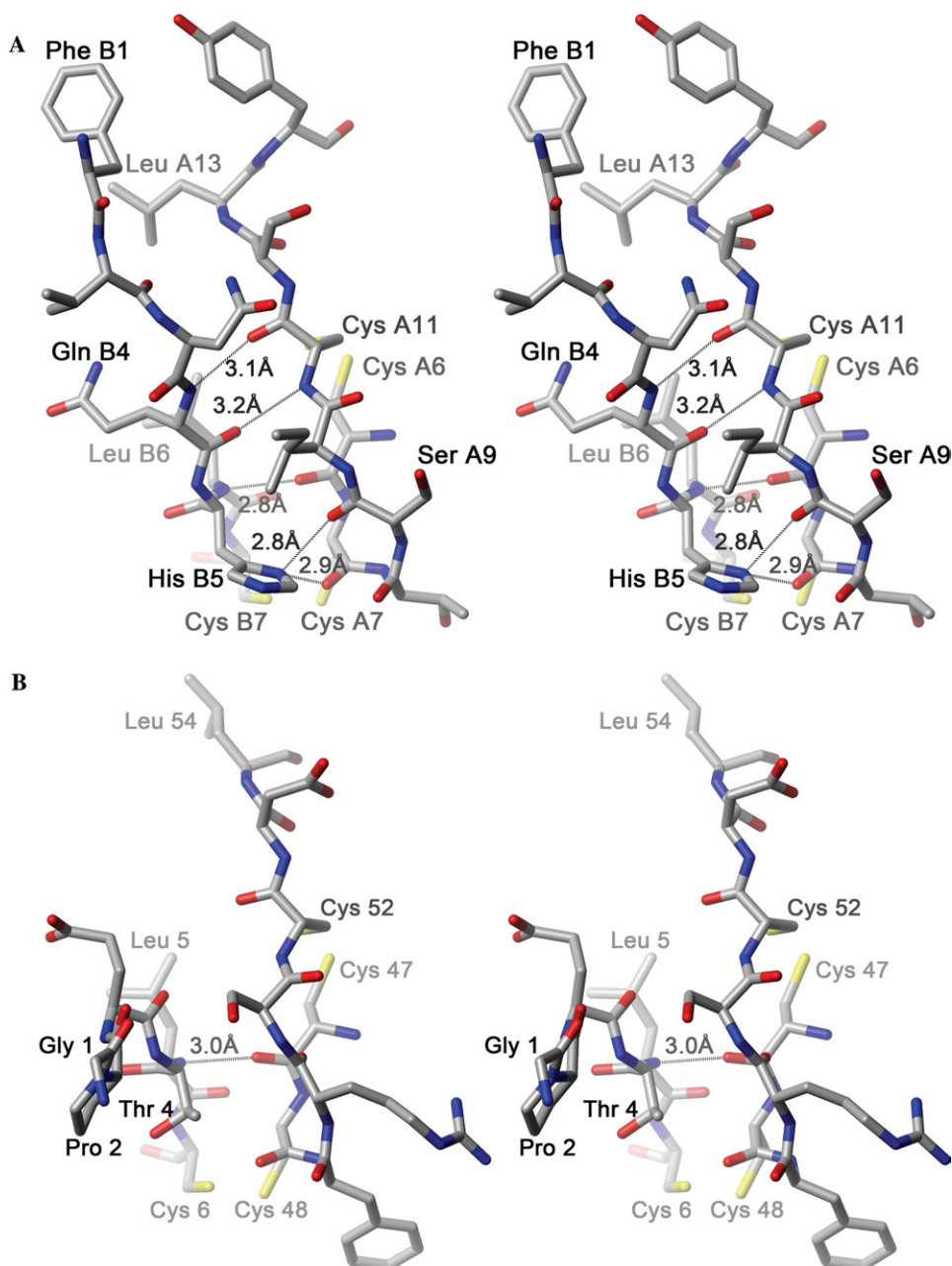


Fig. 3. The hydrogen bonds formed between residues B1–B7 and residues A6–A11 in insulin (stereo view) (A) and the counterpart of IGF-1 (B). It can be seen that in insulin several hydrogen bonds stabilize the conformation of the intra-A-chain disulfide region of the A-chain, while in IGF-1 there is only one hydrogen bond, so the intra-A-chain disulfide is not as stable as that in insulin.

bifurcation in the process of evolution from their common ancestor molecule.

#### *An analysis of the effect of the shortened linker peptides on receptor binding properties*

Site-directed mutagenesis indicated that the main determinants for receptor binding of IGF-1R to IGF-1 and IR lie in the N-terminal region of the A-chain/domain and the  $\beta$ -strand in the C-terminal region of the B-chain/domain [3], among which the key residues for

receptor binding are Phe23, Tyr24, and Phe25 [12]. Bayne et al. [13] demonstrated that IGF-1R also recognizes Tyr31 and Tyr60, of which Tyr31 is located on the C-chain/domain of IGF-1. Gill et al. [14] proposed that, similar to insulin, IGF-1 undergoes a conformational change during interaction with its receptor, including the removal of the C-terminal end of the B-chain/domain to expose the covered A-chain/domain residues. The capability of mini-IGF-1(2) binding to its receptor was analyzed based on the above information.

*The shortened linker peptide confined the movement of the C-terminal of the B-chain/domain, which is disadvantageous for receptor binding*

The linker peptide between the B-chain/domain and A-chain/domain in mini-IGF-1(2) is much shorter than that of native IGF-1. It forms an  $\alpha$ -helix with the last three residues of the B-chain/domain and the first 6 residues of the A-chain/domain (Table 3 and Fig. 4A), which is a relatively stable secondary structure. The results are:

- (1) The C-terminal region of the B-chain is tightened, and it cannot move away from the body of the molecule easily.
- (2) The solvent accessibility of Ile33 and Val34 in the N-terminal of the A-chain/domain (the counterparts in insulin are Ile A2 and Val A3, which are important for receptor binding) is reduced.

These differences between mini-IGF-1(2) and the native IGF-1 may cause the receptor binding capability of mini-IGF-1(2) to decrease greatly compared with that of the native IGF-1.

*The solvent accessibility of the key residues for receptor binding is similar in mini-IGF-1(2) and native IGF-1*

Phe23, Tyr24, and Phe25 are all solvent accessible in native IGF-1, while in small mini-IGF-1 only Tyr24 is fully accessible; Phe25 is much less accessible, and Phe23 is buried deeply in the molecule [15]. This greatly reduces the receptor binding affinity of the molecule to its receptor. Mini-IGF-1(2) is different from small mini-IGF-1 in the accessibility of these key residues. In mini-IGF-1(2), the conformation and accessibility of Phe23 are similar to those of native IGF-1, while Tyr24, and Phe25 show similar accessibility to that of native IGF-1 although their side-chain conformation is a bit different from that of native IGF-1 (Fig. 4B). So we deduced that Phe23, Tyr24, and Phe25 in mini-IGF-1(2) may largely retain their receptor binding activity.

We deduced from the above analysis that although the shortened linker peptide results in great structural changes in mini-IGF-1(2) and some disadvantageous properties for receptor binding (e.g., fixing of the C-terminal conformation of the B-chain/domain), the accessi-

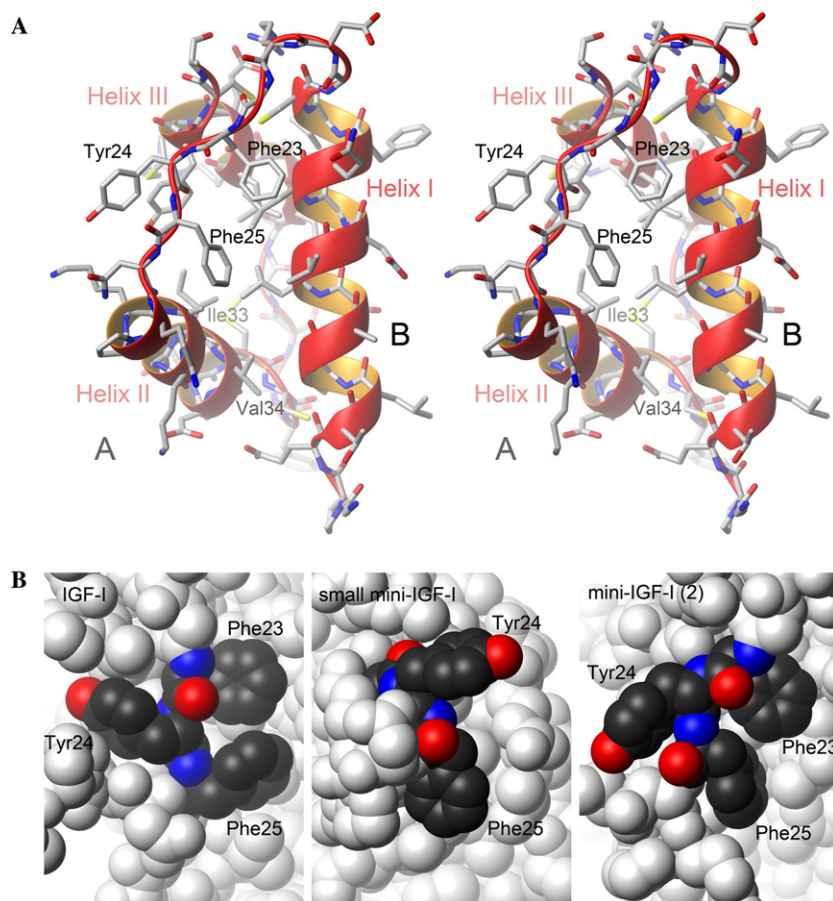


Fig. 4. (A) A stereo view showing the linker peptide region of mini-IGF-1(2). It can be seen clearly that the C-terminal end of the B-chain/domain, the linker peptide, and the N-terminal end of the A-chain/domain form a long  $\alpha$ -helix that stabilizes the conformation of this region and buries Ile33 and Val34 (equivalent to Ile A2 and Val A3 in insulin, which are important for receptor binding). (B) Comparison of the conformation and solvent accessibility of Phe23, Tyr24, and Phe25 in native IGF-1 (left), small mini-IGF-1 (middle), and mini-IGF-1(2) (right).



bility of the key residues needed in receptor binding has been retained to a large extent. Because of this, mini-IGF-1(2)'s receptor binding activity should be retained to some extent and not completely lost as it is in small mini-IGF-1.

## Acknowledgments

We thank Prof. N. Sakabe of the Photon Factory for his assistance in the high resolution dataset collection. And we thank Dr. Tao Jiang for his helpful discussion. This project was financially supported by the National High Technology Research and Development Program (No. 2002BA711A12), the National Natural Science Foundation of China Grants (No. 30130080), the Chinese Academy of Sciences Grants (No. KSCX1-SW-17), and the National Basic Research Program of China (No. 2002CB713801).

## References

- [1] S.J. Moschos, C.S. Mantzoros, The role of the IGF system in cancer: from basic to clinical studies and clinical applications, *Oncology* 63 (2002) 317–332.
- [2] W. Zeslawski, H.G. Beisel, M. Kamionka, W. Kalus, R.A. Engh, R. Huber, K. Lang, T.A. Holak, The interaction of insulin-like growth factor-I with the N-terminal domain of IGFBP-5, *EMBO J.* 20 (2001) 3638–3644.
- [3] J. Murray-Rust, A.N. McLeod, T.L. Blundell, S.P. Wood, Structure and evolution of insulins: implications for receptor binding, *Bioessays* 14 (1992) 325–331.
- [4] R.D. DiMarchi, J.P. Mayer, L. Fan, D.N. Brems, B.H. Frank, L.K. Green, J.A. Hoffmann, D.C. Howey, H.B. Long, W.N. Shaw, J.E. Shields, L.J. Sliker, K.S.E. Su, K.L. Sundell, R.E. Chance, in: J.A. Smith (Ed.), *Peptides: Proceedings of the 12th American Peptide Symposium*, 1992, pp. 26–28.
- [5] Z.Y. Guo, L. Shen, Y.M. Feng, The different folding behavior of insulin and insulin-like growth factor I is mainly controlled by their B-chain/domain, *Biochemistry* 41 (2002) 1556–1567.
- [6] J. Massague, M.P. Czech, The subunit structures of two distinct receptors for insulin-like growth factors I and II and their relationship to the insulin receptor, *J. Biol. Chem.* 257 (1982) 5038–5045.
- [7] A. Ullrich, A. Gray, A.W. Tam, T. Yang-Feng, M. Tsubokawa, C. Collins, W. Henzel, T. Le Bon, S. Kathuria, E. Chen, Insulin-like growth factor I receptor primary structure: comparison with insulin receptor suggests structural determinants that define functional specificity, *EMBO J.* 5 (1986) 2503–2512.
- [8] R.G. Mirmira, H.S. Tager, Role of the phenylalanine B24 side chain in directing insulin interaction with its receptor. Importance of main chain conformation, *J. Biol. Chem.* 264 (1989) 6349–6354.
- [9] D.C. Liang, W.R. Chang, J.P. Zhang, Z.L. Wan, The possible mechanism of binding interaction of insulin molecule with its receptor, *Sci. China B* 35 (1992) 547–557.
- [10] S.H. Nakagawa, H.S. Tager, Importance of aliphatic side-chain structure at positions 2 and 3 of the insulin A chain in insulin-receptor interactions, *Biochemistry* 31 (1992) 3204–3214.
- [11] A. Wollmer, G. Gilge, D. Brandenburg, H.G. Gattner, An insulin with the native sequence but virtually no activity, *Biol. Chem. Hoppe Seyler* 375 (1994) 219–222.
- [12] M.A. Cascieri, G.G. Chicchi, J. Applebaum, N.S. Hayes, B.G. Green, M.L. Bayne, Mutants of human insulin-like growth factor I with reduced affinity for the type 1 insulin-like growth factor receptor, *Biochemistry* 27 (1988) 3229–3233.
- [13] M.L. Bayne, J. Applebaum, G.G. Chicchi, R.E. Miller, M.A. Cascieri, The roles of tyrosines 24, 31, and 60 in the high affinity binding of insulin-like growth factor-I to the type 1 insulin-like growth factor receptor, *J. Biol. Chem.* 265 (1990) 15648–15652.
- [14] R. Gill, B. Wallach, C. Verma, B. Urso, E. De Wolf, J. Grotzinger, J. Murray-Rust, J. Pitts, A. Wollmer, P. De Meyts, S. Wood, Engineering the C-region of human insulin-like growth factor-1: implications for receptor binding, *Protein Eng.* 9 (1996) 1011–1019.
- [15] E. De Wolf, R. Gill, S. Geddes, J. Pitts, A. Wollmer, J. Grotzinger, Solution structure of a mini IGF-1, *Protein Sci.* 5 (1996) 2193–2202.
- [16] E. Girard, M. Stelter, P.L. Anelli, J. Vicat, R. Kahn, A new class of gadolinium complexes employed to obtain high-phasing-power heavy-atom derivatives: results from SAD experiments with hen egg-white lysozyme and urate oxidase from *Aspergillus flavus*, *Acta Crystallogr. D. Biol. Crystallogr.* 59 (2003) 118–126.
- [17] Z. Otwinowski, W. Minor, Processing of X-ray diffraction data collected in oscillation mode, in: C.W. Carter, Jr., R.M. Sweet (Eds.), *Methods in Enzymology*, Volume 276: Macromolecular Crystallography, Part A, Academic Press, San Diego, 1997, pp. 307–326.
- [18] E. de La Fortelle, G. Bricogne, Maximum-likelihood heavy-atom parameter refinement for multiple isomorphous replacement and multiwavelength anomalous diffraction methods, *Methods Enzymol.* 276 (1997) 472–494.
- [19] J.P. Abrahams, A.G. Leslie, Methods used in the structure determination of bovine mitochondrial F1 ATPase, *Acta Crystallogr. D* 52 (1996) 30–42.
- [20] A. Perrakis, R. Morris, V.S. Lamzin, Automated protein model building combined with iterative structure refinement, *Nat. Struct. Biol.* 6 (1999) 458–463.
- [21] G.N. Murshudov, A.A. Vagin, E.J. Dodson, Refinement of macromolecular structures by the maximum-likelihood method, *Acta Crystallogr. D* 53 (1997) 240–255.
- [22] T.A. Jones, J.Y. Zou, S.W. Cowan, M. Kjeldgaard, Improved methods for building protein models in electron density maps and the location of errors in these models, *Acta Crystallogr. A* 47 (Pt. 2) (1991) 110–119.
- [23] S. Hober, G. Forsberg, G. Palm, M. Hartmanis, B. Nilsson, Disulfide exchange folding of insulin-like growth factor I, *Biochemistry* 31 (1992) 1749–1756.
- [24] Z.Y. Guo, L. Shen, Y.M. Feng, The different energetic state of the intra A-chain/domain disulfide of insulin and insulin-like growth factor I is mainly controlled by their B-chain/domain, *Biochemistry* 41 (2002) 10585–10592.
- [25] E.N. Baker, T.L. Blundell, J.F. Cutfield, S.M. Cutfield, E.J. Dodson, G.G. Dodson, D.M. Hodgkin, R.E. Hubbard, N.W. Isaacs, C.D. Reynolds, The structure of 2Zn pig insulin crystals at 1.5 Å resolution, *Philos. Trans. R. Soc. Lond. B Biol. Sci.* 319 (1988) 369–456.
- [26] Y. Chen, Y. You, R. Jin, Z.Y. Guo, Y.M. Feng, Sequences of B-chain/domain 1-10/1-9 of insulin and insulin-like growth factor I determine their different folding behavior, *Biochemistry* 43 (2004) 9225–9233.
- [27] S. Wang, Z.Y. Guo, L. Shen, Y.J. Zhang, Y.M. Feng, Refolding of amphioxus insulin-like peptide: implications of a bifurcating evolution of the different folding behavior of insulin and insulin-like growth factor I, *Biochemistry* 42 (2003) 9687–9693.